

Superconductivity under pressure in $R\text{FeAsO}_{1-x}\text{F}_x$ ($R = \text{La, Ce-Sm}$) by dc magnetization measurements

Kiyotaka Miyoshi, Eiko Kojima, Saki Ogawa, Yuta Shimojo, and Jun Takeuchi

Department of Material Science, Shimane University, Matsue 690-8504, Japan

(Received 4 March 2013; published 11 June 2013)

Superconducting transition under pressure (P) has been investigated for optimum-doped $R\text{FeAsO}_{1-x}\text{F}_x$ ($R = \text{La, Ce-Sm}$) by dc magnetization measurements. For $R = \text{La}$, T_c is found to be pressure independent up to $P \sim 3.0$ GPa and then shows a monotonic decrease with increasing pressure. The plateau width decreases for the system with smaller lattice constants and shrinks to almost zero for $R = \text{Sm}$. From the $T_c(P)$ data, we construct the T_c evolution map on the height of the As atom from the Fe-plane h_{As} versus lattice-constant a or c plane. It is shown that the characteristic T_c variations under pressure for all compounds and the rapid decrease in T_c induced by changing the R element from Sm to La can be described by a common $T_c(h_{\text{As}}, a \text{ or } c)$ surface, suggesting that T_c is determined by h_{As} and lattice constant. It is also suggested that there exists an upper limit of the lattice constant a_{ulm} (or c_{ulm}), above which dT_c/da (or dT_c/dc) changes the sign from positive to negative.

DOI: [10.1103/PhysRevB.87.235111](https://doi.org/10.1103/PhysRevB.87.235111)

PACS number(s): 74.70.Xa, 74.62.Fj

I. INTRODUCTION

Since the discovery of superconductivity in $\text{LaFeAsO}_{1-x}\text{F}_x$ ($T_c = 26$ K),¹ a great deal of progress has been made in exploring superconductivity in the related compounds, leading to a rich variety of iron-pnictide superconductors, such as $\text{Ba}_{1-x}\text{K}_x\text{Fe}_2\text{As}_2$ ($T_c = 38$ K),^{2,3} $\text{Li}_{1-x}\text{FeAs}$ ($T_c = 18$ K),^{4,5} FeSe ($T_c = 8$ K),⁶ and $\text{K}_{0.8}\text{Fe}_2\text{Se}_2$ ($T_c = 32$ K),⁷ in addition to $R\text{FeAsO}_{1-x}\text{F}_x$ ($R = \text{lanthanoid}$) ($T_c = 26\text{--}53$ K), where the superconductivity is developed in iron-pnictide (Fe-Pn) layers consisting of edge-sharing FePn_4 tetrahedron. Indeed, there exists an intimate correlation between the crystal structure and T_c in the iron-pnictide family, as demonstrated in $R\text{FeAsO}_{1-x}\text{F}_x$ that T_c becomes maximum when FeAs_4 forms a regular tetrahedron, i.e., the As-Fe-As bond angle is $\sim 109.5^\circ$.⁸ Also, the pnictogen height h_{Pn} measured from the Fe plane is known to be an important structural parameter, which is originally introduced to act as a switch between high- T_c state with nodeless paring to low- T_c state with nodal paring.⁹ There are some attempts to plot T_c versus h_{Pn} for typical iron-pnictide superconductors, suggesting that the data collapse to a universal curve.^{10,11}

Application of pressure can induce the modification of the crystal structure leading to the change in T_c . Thus, to obtain the intrinsic relation between T_c and structural parameters under pressure is of significant importance, providing valuable information to elucidate the mechanism of superconductivity. One of the attractive subjects for studying the pressure effect is $R\text{FeAsO}_{1-x}\text{F}_x$, where T_c systematically changes by replacing the R element, so that we can extract more information by comparing the variations of T_c induced by physical and chemical pressure to specify which parameters play a crucial role for the superconductivity.

The pressure effect for $R\text{FeAsO}_{1-x}\text{F}_x$ has been investigated by many researchers through the measurements of electrical resistivity (ρ),^{12–20,22–26} ac and dc magnetization,^{27–31} x-ray diffraction,^{19,26,32} NMR,^{23,33} and others.^{20,31} For $\text{LaFeAsO}_{1-x}\text{F}_x$ with $x = 0.11$, it has been suggested that T_c increases with increasing pressure P and shows a maximum of 43 K at $P \sim 4$ GPa through the $\rho(T)$ measurements by determining T_c from the onset of resistive drop.^{12,13} In the

study, if T_c is determined by the zero resistive temperature, which is fairly lower than the onset, the T_c - P curve would be a quite different one showing a gradual increase from ~ 23 to ~ 28 K for $0 \leq P \leq 3$ GPa.¹² Since the resistivity drop usually occurs over a wide temperature range when the polycrystalline sample is used, it is extremely difficult to determine T_c precisely only by the $\rho(T)$ data. Magnetization data, by which T_c is determined solely from diamagnetic onset, should be used together with $\rho(T)$ data. However, to our knowledge, the magnetic measurements for $R\text{FeAsO}_{1-x}\text{F}_x$ have been limited to the low-pressure range below ~ 1 GPa.^{27–31}

In the present work, we have performed dc magnetization measurements for optimum-doped $R\text{FeAsO}_{1-x}\text{F}_x$ ($R = \text{La, Ce-Sm}$) under pressure using a diamond anvil cell (DAC) to establish the T_c - P relation. Our dc magnetic measurement using DAC is a powerful technique to determine T_c under pressure and has been successfully applied to other superconductors.^{34,35} In this paper, it is found that the T_c - P curve for $R = \text{La}$ is pressure independent up to ~ 3.0 GPa and decreases monotonically above 3 GPa. The plateau width becomes narrower for the system with smaller lattice constants and almost shrinks to zero for $R = \text{Sm}$. These behaviors, and also the T_c variation induced by the chemical substitution, can be explained by considering the effect of the As height h_{As} and the lattice constant on T_c together with an upper limit of the lattice constant, across which dT_c/da (or dT_c/dc) changes the sign.

II. EXPERIMENTAL

The polycrystalline samples of optimum-doped $R\text{FeAsO}_{1-x}\text{F}_x$ ($R = \text{La, Ce-Sm}$) were synthesized by a solid-state reaction technique³⁶ heating the pelletized mixtures of $R\text{As}$, Fe, Fe_2O_3 , and FeF_2 powders at 1100°C for 20 h. The pellet was wrapped with Ta foil and put in an evacuated silica tube. $R\text{As}$ was prepared by reacting R and As powders in an evacuated silica tube at $250\text{--}1000^\circ\text{C}$, as described in the literature.³⁷ All operations for the synthesis were carried out in an Ar atmosphere. The samples were confirmed to be a single phase by x-ray diffraction. For the optimum doping, our specimens were prepared with nominal

fluorine content x ranging from 0.1 to 0.2. T_c of our specimens determined by the diamagnetic onset at ambient pressure was ~ 27 K ($R = \text{La}$), ~ 38 K (Ce), ~ 43 K (Pr), ~ 48 K (Nd), and ~ 53 K (Sm), consistent with the previous reports.^{38–41} For the magnetic measurements under high pressure, a miniature DAC with an outer diameter of 8 mm was used to generate high pressure and combined with a sample rod of a commercial superconducting quantum interference device magnetometer. The details of the DAC are given elsewhere.⁴² The sample was loaded into the gasket hole together with a small piece of high-purity lead (Pb) to realize the *in situ* observation of pressure by determining the pressure from the T_c shift of Pb . Magnetization data for the small amounts of $R\text{FeAsO}_{1-x}\text{F}_x$ and Pb were obtained by subtracting the magnetic contribution of DAC measured in an empty run from the total magnetization data. Daphne oil 7373 was used as a pressure transmitting medium. For the measurements in the high-pressure regime, liquid Ar was also used to apply hydrostatic pressure.

III. RESULTS

In this section, we show typical zero-field cooled dc magnetization (M) versus temperature (T) curves for $R = \text{La}$ and Ce-Sm under various pressures. T_c was determined by the onset temperature of diamagnetic response in the M - T curve. The onset temperature was estimated by extrapolating the initial slope of the M - T curve just below T_c to the normal state magnetization. Figure 1(a) shows the M - T curves at low pressures below 3.5 GPa for $R = \text{La}$. At ambient pressure, the M - T curve exhibits a sudden decrease at ~ 28 K, indicating the onset of the diamagnetic response accompanied by the superconducting transition at $T_c \sim 28$ K. For $0 \leq P \leq 2.4$ GPa, the onset temperature does not appear to change, indicating that T_c is pressure independent. Above 3.1 GPa,

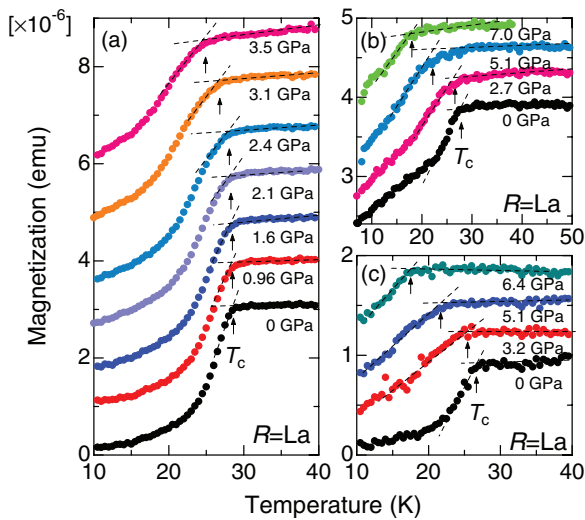


FIG. 1. (Color online) Temperature dependence of zero-field-cooled dc magnetization measured with a magnetic field of $H = 20$ Oe under various pressures up to (a) 3.5 GPa, (b) 7.0 GPa, and (c) 7.5 GPa for $\text{LaFeAsO}_{1-x}\text{F}_x$. The data are intentionally shifted along the longitudinal axis for clarity. The data measured using liquid Ar as a pressure transmitting medium are shown in (c).

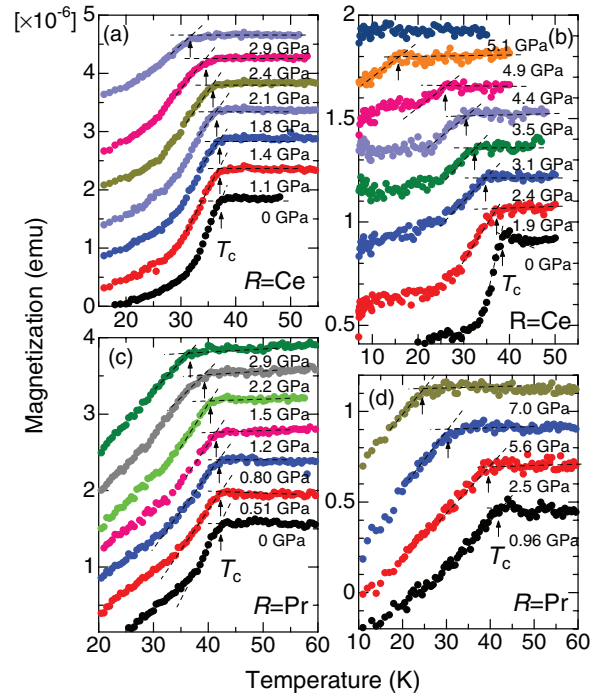


FIG. 2. (Color online) Temperature dependence of zero-field-cooled dc magnetization measured with a magnetic field of $H = 20$ Oe under various pressures up to (a) 2.9 GPa and (b) 5.1 GPa for $\text{CeFeAsO}_{1-x}\text{F}_x$ and (c) 2.9 GPa and (d) 7.0 GPa for $\text{PrFeAsO}_{1-x}\text{F}_x$. The data are intentionally shifted along the longitudinal axis for clarity. The data measured using liquid Ar as a pressure transmitting medium are shown in (b) and (d).

T_c is found to gradually shift to the lower-temperature side. In Figs. 1(b) and 1(c), we show the typical M - T curves at higher pressures. As pressure increases, T_c decreases slowly and reaches ~ 18 K at $P = 7.0$ GPa. Next, we show the typical M - T curves for $R = \text{Ce}$ and Pr in Figs. 2(a)–2(d). For $R = \text{Ce}$, a sharp diamagnetic response is seen at ambient pressure below $T_c \sim 38$ K, but T_c is unchanged at least up to $P = 1.4$ GPa, similar to the behavior seen for $R = \text{La}$, and then decreases gradually above $P = 1.8$ GPa, as seen in Fig. 2(a). In Fig. 2(b), T_c is found to be 25 K at $P = 4.4$ GPa, above which T_c , however, rapidly decreases with increasing pressure, and diamagnetic response was not observed at $P = 5.1$ GPa above 5 K, suggesting that the superconductivity is suppressed under pressure above 5 GPa. Disappearance of superconductivity under pressure for $R = \text{Ce}$ has been previously reported in earlier studies,^{21,22,24} where the origin is discussed in terms of the valence transition of Ce ion and the competition between superconductivity and the Kondo screening state.

In Fig. 2(c), both of the M - T curves for $R = \text{Pr}$ at ambient pressure and at $P = 0.51$ GPa indicate a superconducting transition at $T_c \sim 43$ K. Above $P = 0.80$ GPa, T_c begins to shift toward the lower-temperature side, indicating that T_c is nearly constant in the pressure range below 0.8 GPa, which is lower than that observed for $R = \text{La}$ and Ce . With further pressure increase, T_c for $R = \text{Pr}$ shows a monotonic decrease and reaches ~ 25 K at 7.0 GPa, as seen in Fig. 2(d). Figures 3(a)–3(d) show the M - T curves for $R = \text{Nd}$ and Sm . T_c for $R = \text{Nd}$ appears to be ~ 48 K at $P = 0.39$ GPa in Fig. 3(a).

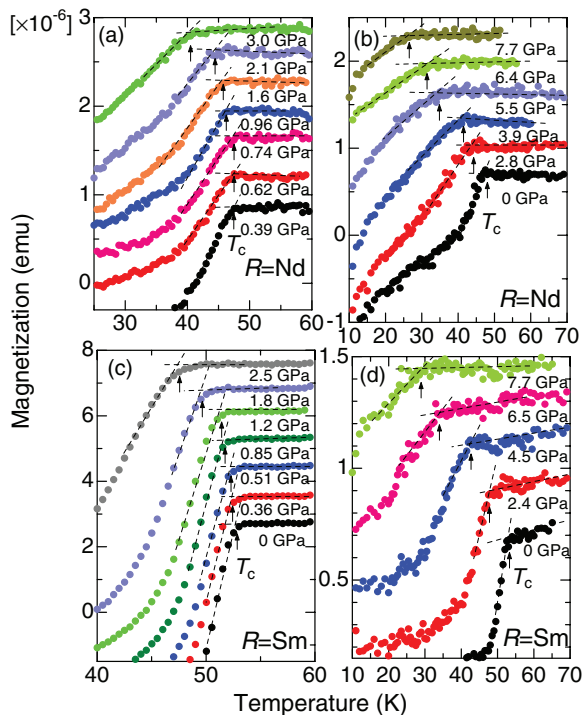


FIG. 3. (Color online) Temperature dependence of zero-field-cooled dc magnetization measured with a magnetic field of $H = 20$ Oe under various pressures up to (a) 3.0 GPa and (b) 7.7 GPa for NdFeAsO_{1-x}F_x and up to (c) 2.5 GPa and (d) 7.7 GPa for SmFeAsO_{1-x}F_x. The data are intentionally shifted along the longitudinal axis for clarity. The data measured using liquid Ar as a pressure transmitting medium are shown in (d).

A remarkable shift of T_c is not observed up to $P = 0.74$ GPa but further application of pressure suppresses T_c down to 26 K at $P = 7.7$ GPa, as seen in Fig. 3(b). The pressure range in which T_c is pressure independent is similar to that for $R = \text{Pr}$. On the other hand, it is found that the diamagnetic onset in the M - T curve for $R = \text{Sm}$ at 0.36 GPa is slightly lowered from that at ambient pressure (~ 53 K) and then monotonously decreased down to ~ 48 K at 2.5 GPa and ~ 29 K at 7.7 GPa by the application of pressure, as seen in Figs. 3(c) and 3(d). T_c for $R = \text{Sm}$ is immediately decreased without delay even in the low-pressure region.

Next, we show plots of T_c versus P data for $R = \text{La}$ and Ce-Sm in Fig. 4. In the figure, a characteristic plateau is seen in the T_c - P curve for $R = \text{La}$ in the pressure range below $P_w \sim 3.0$ GPa. For the system with a smaller lattice constant, the plateau width in the T_c - P curve is found to be narrower, i.e., $P_w \sim 1.5$ GPa for $R = \text{Ce}$, $P_w \sim 0.5 - 1.0$ GPa for $R = \text{Pr}$ and Nd, and $P_w < 0.5$ GPa for $R = \text{Sm}$. For $P \geq P_w$, the T_c - P curve exhibits a monotonic decrease except for $R = \text{Ce}$. T_c for $R = \text{Ce}$ decreases rapidly, especially above $P = 4$ GPa, dropping toward $T_c = 0$ at $P = 5$ GPa. The decreasing rates dT_c/dP for $R = \text{Pr-Sm}$ are similar to each other, yielding -3 to -4 K/GPa. In the figure, it is also found that the T_c - P relation does not depend on whether the pressure transmitting medium is liquid Ar or Daphne oil 7373.

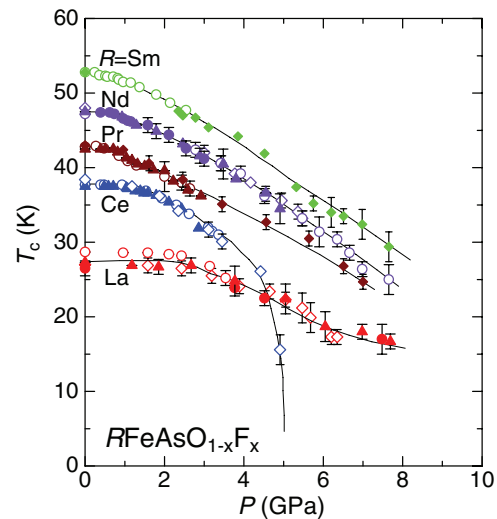


FIG. 4. (Color online) Pressure variations of critical temperature T_c for RFeAsO_{1-x}F_x ($R = \text{La, Ce-Sm}$). The solid lines are guides for the eyes. The data sets measured in different runs are plotted by different symbols. Open and closed diamonds (other symbols) indicate the data obtained by using liquid Ar (Daphne oil 7373) as the pressure transmitting medium.

IV. DISCUSSION

A. Intrinsic T_c - P relation

One may note that the plateau behavior in the T_c - P curve for $R = \text{La}$ seen in Fig. 4 is inconsistent with the T_c - P relation reported by Takahashi *et al.*, which is determined from the onset of resistive drop for the specimen with F content $x = 0.11$, showing a maximum of $T_c \sim 43$ K at $P \sim 4$ GPa.¹² The discrepancy originates from not only the difference in the definition of T_c but also the difference in the doping level of the specimens, because their specimen with $x = 0.11$ shows a relatively low diamagnetic onset temperature of ~ 22 K at ambient pressure.¹² On the other hand, T_c for their specimen with $x = 0.05$ is ~ 23 K,¹² and T_c for $x = 0.08$ is found to be ~ 28 K,²³ indicating that their specimen with $x = 0.11$ (0.08) is overdoped (optimally doped). For $x = 0.08$, it has been shown that the zero resistive temperature in the $\rho(T)$ curve (~ 28 K) is unchanged at least up to 2.60 GPa.²³ The behavior is the same with that observed for $R = \text{La}$, as shown in the T_c - P curve in Fig. 4, indicating that the zero resistive temperature and the diamagnetic onset are identical to each other, and both of them can be reliable markers of T_c for RFeAsO_{1-x}F_x. We therefore suggest that the behavior showing a plateau for $0 \leq P \leq 3$ GPa is the intrinsic T_c - P relation for optimally doped $R = \text{La}$.

Pressure dependence of T_c has been widely investigated by the $\rho(T)$ and $M(T)$ measurements for $R = \text{Sm}$,^{15,17,26,28,30} Nd,¹⁴ Pr,³⁰ and Ce,^{16,22,24} and negative pressure coefficients of T_c have been found in these studies. In particular, the investigations in the high-pressure range have been done by the $\rho(T)$ measurements adopting the onset temperature of resistive drop as T_c for $R = \text{Sm}$ and Nd, resulting in $dT_c/dP \sim -3.0$ K/GPa.^{14,26} The value is similar to that obtained for $R = \text{Sm-Pr}$ in the present study. For $R = \text{Ce}$, the T_c - P relation has been also investigated through the $\rho(T)$

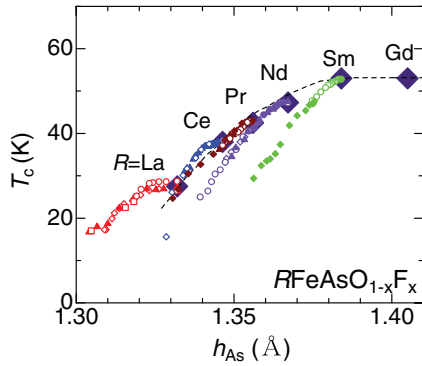


FIG. 5. (Color online) Plots of T_c vs height of the As layer from Fe layer h_{As} for $RFeAsO_{1-x}F_x$ ($R = La, Ce-Sm$). The broken line interpolates the data at ambient pressure, which are displayed by large closed diamonds, and corresponds to the variation for the chemical substitution for the R site. Small symbols represent the data obtained from the physical pressure dependence of T_c . The $T_c(P)$ data are transformed to $T_c(h_{As})$ data assuming a linear relation with a coefficient $dh_{As}/dP \sim -3.6 \times 10^{-3} \text{ Å GPa}^{-1}$ extracted from the pressure variations of structural parameters in the literature.²⁶ The values of h_{As} at ambient pressure can be obtained from the literature.^{8,11,44,45}

measurements, suggesting that the superconductivity disappears at $P = 4.5-5 \text{ GPa}$,²⁴ similar to the result shown in Fig. 4.

B. Plots of T_c versus h_{As}

Pnictogen height from the Fe-layer h_{pn} is considered to be a key factor to determine T_c in an iron-pnictide superconductor. For FeSe superconductor, it has been found that the pressure variations of T_c and Se height h_{Se} are qualitatively analogous to each other.¹¹ Also, for $SmFeAsO_{1-x}F_x$, an attempt to compare the pressure variations of T_c and h_{As} has been made, confirming that both of them show a monotonous decrease under pressure above 1 GPa.²⁶ As shown theoretically, the increase of h_{As} leads to the appearance of the γ Fermi surface, resulting in the enhancement of T_c (i.e., $dT_c/dh_{As} > 0$) in $RFeAsO$ system.⁹ In order to examine the importance of h_{As} , it is interesting to compare the T_c versus h_{As} data derived from the structural modulation originating from the physical compression and the chemical substitution for R site. If h_{As} is the only structural parameter to determine T_c , the T_c-h_{As} data under physical and chemical pressure would coincide with each other. To obtain $T_c(h_{As})$ data, we transform the $T_c(P)$ data assuming a linear relation between h_{As} and P with a coefficient $dh_{As}/dP \sim -3.6 \times 10^{-3} \text{ Å GPa}^{-1}$, which is extracted from the pressure variations of structural parameters for $SmFeAsO_{1-x}F_x$ interpolating the data for $0.5 \leq P \leq 20 \text{ GPa}$ in the literature.²⁶ The value of dh_{As}/dP well agrees with that obtained from the first-principles calculations of the pressure effect on $LaFeAsO$, that is $dh_{As}/dP \sim -3.5 \times 10^{-3} \text{ Å GPa}^{-1}$.⁴³

In Fig. 5, we show the plots of T_c versus h_{As} . The T_c-h_{As} curve for the chemical substitution for R site (the broken line) is flat in the high h_{As} side, and even in the higher h_{As} region it is flat because T_c at ambient pressure is known to be 52–53 K for $R = Sm-Dy$.⁴⁶ In contrast, T_c rapidly decreases in the low h_{As} region below the value for $R = Sm$. The $T_c(h_{As})$ data for

the physical compression for $R = Sm$ in Fig. 5 are found to be not coincident with the broken line, showing a rapid decrease with decreasing h_{As} . For $R = Gd$ and Tb , T_c is known to decrease monotonically with increasing pressure, similar to that for $R = Sm$.⁴⁷ Since T_c is nearly constant for $R = Sm-Dy$ at ambient pressure, the $T_c(h_{As})$ data under pressure for $R = Gd$ and Tb are expected to be not coincident with the broken line. In addition, a constant part in the $T_c(h_{As})$ data for $R = La$, corresponding to the T_c-P plateau, is also not reproduced by the broken line. The discrepancies between the T_c-h_{As} relations coming from the physical compression and the chemical substitution indicate that T_c is determined not only by h_{As} but also by another structural parameter.

C. T_c evolution on h_{As} -lattice-constant plane

Kuroki *et al.* have pointed that the reduction of the lattice constant a or c suppresses superconductivity in $RFeAsO$ (i.e., $dT_c/da > 0$ or $dT_c/dc > 0$) due to the increased hopping integrals and the associated suppression of the electron correlation, and therefore the lattice constant is also an important parameter to determine T_c .⁹ It should be noted that the lattice constant increases when h_{As} is decreased by the chemical substitution but it decreases when h_{As} is decreased by the physical compression, changing in opposite directions. This could be the origin of the difference in the T_c-h_{As} relations derived from the physical compression and the chemical substitution if T_c also depends on the lattice constant. Kuroki *et al.* have also suggested that the effects of h_{As} and the lattice constant on T_c may cancel with each other to result in a nearly constant T_c between $R = Nd-Dy$ at ambient pressure.⁹ This idea lead us to expect the existence of an upper limit of the lattice constant near the value for $R = Sm$, above which dT_c/da (or dT_c/dc) changes the sign from positive to negative, leading to the rapid decrease in T_c from 53 K ($R = Sm$) to 27 K ($R = La$) due to the combined effect of $dT_c/dh_{As} > 0$ and $dT_c/da < 0$ ($dT_c/dc < 0$). The plateau in the T_c-P curve observed in the low-pressure region can be also explained by the existence of the upper limit of the lattice constant. When the lattice constant is larger than the limit at low pressure, the effect of $dT_c/dh_{As} > 0$ decreases T_c with increasing pressure, whereas the effect of $dT_c/da < 0$ (or $dT_c/dc < 0$) increases T_c with increasing pressure. The cancellation of these effects can be the origin of the pressure independent behavior of T_c .

In order to confirm the importance of h_{As} and lattice constant for the superconductivity in $RFeAsO_{1-x}F_x$, and also the existence of the upper limit of the lattice constant, we show T_c evolution on the h_{As} -lattice-constant plane in Figs. 6(a) and 6(b). For the construction of the evolution maps, $T_c(P)$ data were transformed to $T_c(h_{As}, a)$ and $T_c(h_{As}, c)$ data, assuming the same linear relations for all compounds, $a = -9.3 \times 10^{-3} P + a(0)$ and $c = -4.7 \times 10^{-2} P + c(0)$, obtained using the data in the low-pressure range ($P \leq 8 \text{ GPa}$) in the literature,¹⁹ in addition to $h_{As} = -3.6 \times 10^{-3} P + h_{As}(0)$,²⁶ although the relations should be estimated individually using the structural data for each compound for the more exact construction. Then, $T_c(h_{As}, a$ or $c)$ data were plotted and the contours of T_c (solid lines) were drawn by connecting the data points with similar T_c . The data points (small symbols) on the plane represent that both h_{As} and lattice constant for

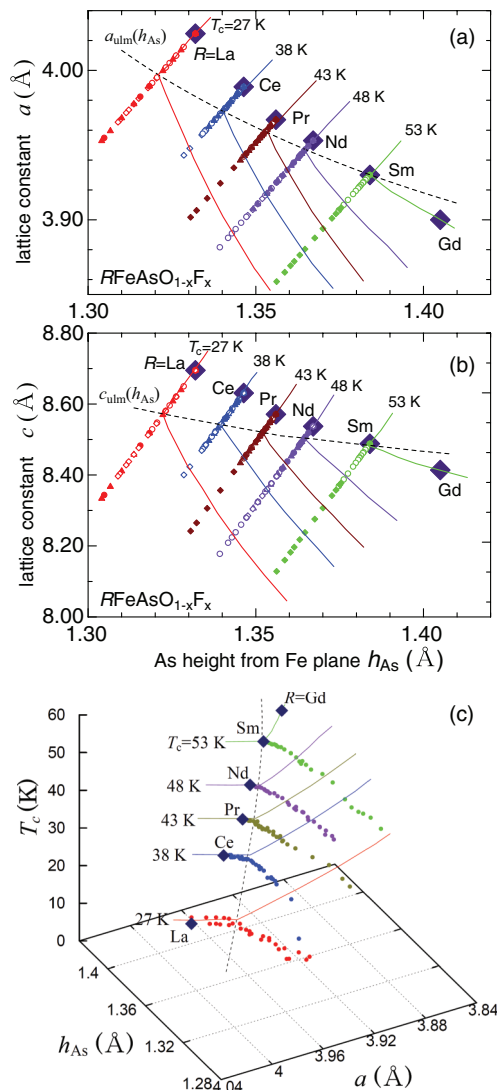


FIG. 6. (Color online) T_c evolution on the h_{As} -lattice-constant (a) a and (b) h_{As} - c planes for $R\text{FeAsO}_{1-x}\text{F}_x$. The $T_c(P)$ data for each system are plotted on the planes after transforming the data, assuming linear relations $h_{\text{As}} = -3.6 \times 10^{-3} P + h_{\text{As}}(0)$, $a = -9.3 \times 10^{-3} P + a(0)$, and $c = -4.7 \times 10^{-2} P + c(0)$ obtained from the literature.^{19,26} The data at ambient pressure for $R = \text{La, Ce-Gd}$ are displayed by large closed diamonds. The solid lines indicate contours of T_c , which are drawn by connecting the data point with similar T_c . The broken line indicates the upper limit of the lattice constant $a_{\text{ulm}}(h_{\text{As}})$ ($c_{\text{ulm}}(h_{\text{As}})$), above which dT_c/da (dT_c/dc) changes the sign from positive to negative. (c) Three-dimensional plots of T_c as a function of h_{As} and a . The solid lines (broken line) indicate(s) contours (a ridge) of the $T_c(h_{\text{As}}, a)$ surface.

each system decrease under pressure from the value at ambient pressure (large closed diamonds). The data points above the broken line coincide with the contour of T_c , corresponding to the T_c - P plateau. The contour of T_c changes the direction across the broken line, indicating that dT_c/da (or dT_c/dc) changes the sign across the line. Therefore, the broken line corresponds to the upper limit of the lattice constant a_{ulm} (c_{ulm}), which we expect as discussed in the previous paragraph. The value of a_{ulm} (c_{ulm}) is different for each system, depending on h_{As} . The qualitative feature of the T_c evolution below the a_{ulm}

(c_{ulm}) line is consistent with that proposed by Kuroki *et al.*⁹ In Fig. 6(c), we show three-dimensional plots of $T_c(h_{\text{As}}, a)$. In the figure, the $T_c(h_{\text{As}}, a)$ surface is described by contours of T_c (solid lines) and a ridge of the surface (broken line). The evolution map of T_c in Fig. 6(a) is a projection of the $T_c(h_{\text{As}}, a)$ surface on the h_{As} - a plane, so that the a_{ulm} line is corresponding to the projection of the ridge of the surface.

We have shown in Fig. 5 that the variations of T_c derived from the physical compression and the chemical substitution cannot be expressed by a universal function $T_c(h_{\text{As}})$. On the other hand, the $T_c(h_{\text{As}}, a$ or $c)$ surface shown in Figs. 6(a)–6(c) can reasonably describe the characteristic variations of T_c , i.e., the T_c - P plateau followed by the monotonic decrease under pressure and the rapid decrease in T_c (nearly constant T_c) by changing R elements from Sm to La (from Tb to Sm). Furthermore, the $T_c(h_{\text{As}}, a$ or $c)$ surface would also describe a monotonic decrease in T_c under pressure observed for $R = \text{Gd}$ and Tb.⁴⁷ These facts suggest that h_{As} and the lattice constant are important structural parameters to determine the superconductivity in $R\text{FeAsO}_{1-x}\text{F}_x$. It is, however, unclear which of the lattice constants is dominant for the superconductivity. The in-plane electron hopping, which is intuitively expected to be essential to the superconductivity due to the layered structure, can be decreased by the enhancement of either a or c .⁹ The electron transfer in the c direction may be also important in view of the doping from the $R\text{-O}_{1-x}\text{F}_x$ layer to the superconducting Fe-As layer. The dc magnetic measurements under uniaxial pressure using single-crystal specimens are necessary to specify the axis sensitive to the superconductivity.

V. SUMMARY

In the present work, we have performed the dc magnetization measurements under pressure for optimally doped $R\text{FeAsO}_{1-x}\text{F}_x$ ($R = \text{La}$ and Ce–Sm). It is found that the T_c - P curve for $R = \text{La}$ exhibits a plateau at the low-pressure range up to ~ 3 GPa, followed by a monotonic decrease at higher pressure. The plateau width in the T_c - P curve is found to depend on the lattice constant of the system and shrinks to nearly zero for $R = \text{Sm}$. Although h_{As} is known to be an important structural parameter, the variations of T_c derived from the physical compression and chemical substitution for R site cannot be expressed by a universal function $T_c(h_{\text{As}})$. Instead, we present the T_c evolution map on the h_{As} -lattice-constant plane, where it is shown that the $T_c(h_{\text{As}}, a$ or $c)$ surface can describe all of the characteristic T_c variations, suggesting that T_c is determined by h_{As} and lattice constant. In addition, the upper limit of the lattice constant a_{ulm} or c_{ulm} , across which dT_c/da (or dT_c/dc) changes the sign, has been shown to exist. The T_c - P plateau observed for $R = \text{La}$ and Ce–Nd is thought to be originating from the effects of h_{As} and lattice constant on T_c canceling each other for $a > a_{\text{ulm}}$ ($c > c_{\text{ulm}}$).

ACKNOWLEDGMENTS

This work is financially supported in part by a Grant-in-Aid for Scientific Research (grant no. 20540355) from the Japanese Ministry of Education, Culture, Sports, Science, and Technology.

- ¹Y. Kamihara, T. Watanabe, M. Hirano, and H. Hosono, *J. Am. Chem. Soc.* **130**, 3296 (2008).
- ²M. Rotter, M. Tegel, and D. Johrendt, *Phys. Rev. Lett.* **101**, 107006 (2008).
- ³K. Sasmal, B. Lv, B. Lorenz, A. M. Guloy, F. Chen, Y. Y. Xue, and C. W. Chu, *Phys. Rev. Lett.* **101**, 107007 (2008).
- ⁴J. H. Tapp, Z. Tang, B. Lv, K. Sasmal, B. Lorenz, P. C. W. Chu, and A. M. Guloy, *Phys. Rev. B* **78**, 060505(R) (2008).
- ⁵X. C. Wang, Q. Q. Liu, Y. X. Lv, W. B. Gao, L. X. Yang, R. C. Yu, F. Y. Li, and C. Q. Jin, *Solid State Commun.* **148**, 538 (2008).
- ⁶F.-C. Hsu, J.-Y. Luo, K.-W. Yeh, T.-K. Chen, T.-W. Huang, P. M. Wu, Y.-C. Lee, Y.-L. Hung, Y.-Y. Chu, D.-C. Yan, and M.-K. Wu, *Proc. Natl. Acad. Sci. USA* **105**, 14262 (2008).
- ⁷J. Guo, S. Jin, G. Wang, S. Wang, K. Zhu, T. Zhou, M. He, and X. Chen, *Phys. Rev. B* **82**, 180520 (2010).
- ⁸C.-H. Lee, A. Iyo, H. Eisaki, H. Kito, M. T. Fernandez-Diaz, T. Ito, K. Kihou, H. Matsuhata, M. Braden, and K. Yamada, *J. Phys. Soc. Jpn.* **77**, 083704 (2008).
- ⁹K. Kuroki, H. Usui, S. Onari, R. Arita, and H. Aoki, *Phys. Rev. B* **79**, 224511 (2009).
- ¹⁰Y. Mizuguchi, Y. Hara, K. Deguchi, S. Tsuda, T. Yamaguchi, K. Takeda, H. Kotegawa, H. Tou, and Y. Takano, *Supercond. Sci. Technol.* **23**, 0540131 (2010).
- ¹¹H. Okabe, N. Takeshita, K. Horigane, T. Muranaka, and J. Akimitsu, *Phys. Rev. B* **81**, 205119 (2010).
- ¹²H. Takahashi, K. Igawa, K. Arii, Y. Kamihara, M. Hirano, and H. Hosono, *Nature (London)* **453**, 376 (2008).
- ¹³H. Okada, K. Igawa, H. Takahashi, Y. Kamihara, M. Hirano, H. Hosono, K. Matsubayashi, and Y. Uwatoko, *J. Phys. Soc. Jpn.* **77**, 113712 (2008).
- ¹⁴N. Takeshita, A. Iyo, H. Eisaki, H. Kito, and T. Ito, *J. Phys. Soc. Jpn.* **77**, 075003 (2008).
- ¹⁵B. Lorenz, K. Sasmal, R. P. Chaudhury, X. H. Chen, R. H. Liu, T. Wu, and C. W. Chu, *Phys. Rev. B* **78**, 012505 (2008).
- ¹⁶D. A. Zocco, J. J. Hamlin, R. E. Baumbach, M. B. Maple, M. A. McGuire, A. S. Sefat, B. C. Sales, R. Jin, D. Mandrus, J. R. Jerjes, S. T. Weir, and Y. K. Vohra, *Physica C* **468**, 2229 (2008).
- ¹⁷W. Yi, L. Sun, Z. Ren, W. Lu, X. Dong, H. Zhang, X. Dai, Z. Fang, Z. Li, G. Che, J. Yang, X. Shen, F. Zhou, and Z. Zhao, *Euro. Phys. Lett.* **83**, 57002 (2008).
- ¹⁸W. Yi, C. Zhang, L. Sun, Z. Ren, W. Lu, X. Dong, Z. Li, G. Che, J. Yang, X. Shen, X. Dai, Z. Fang, F. Zhou, and Z. Zhao, *Euro. Phys. Lett.* **84**, 67009 (2008).
- ¹⁹G. Garbarino, P. Toulemonde, M. Álvarez-Murga, A. Sow, M. Mezouar, and M. Núñez-Regueiro, *Phys. Rev. B* **78**, 100507(R) (2008).
- ²⁰T. Kawakami, T. Kawatani, H. Okada, H. Takahashi, S. Nasu, Y. Kamihara, M. Hirano, and H. Hosono, *J. Phys. Soc. Jpn.* **78**, 123703 (2009).
- ²¹N. Takeshita, K. Miyazawa, A. Iyo, H. Kito, and H. Eisaki, *J. Phys. Soc. Jpn.* **78**, 065002 (2009).
- ²²L. Sun, X. Dai, C. Zhang, W. Yi, G. Chen, N. Wang, L. Zheng, Z. Jiang, X. Wei, Y. Huang, J. Yang, Z. Ren, W. Lu, X. Dong, G. Che, Q. Wu, H. Ding, J. Liu, T. Hu, and Z. Zhao, *Euro. Phys. Lett.* **91**, 57008 (2010).
- ²³T. Nakano, N. Fujiwara, K. Tatsumi, H. Okada, H. Takahashi, Y. Kamihara, M. Hirano, and H. Hosono, *Phys. Rev. B* **81**, 100510(R) (2010).
- ²⁴H. Yamaoka, I. Jarrige, A. Ikeda-Ohno, S. Tsutsui, J.-F. Lin, N. Takeshita, K. Miyazawa, A. Iyo, H. Kito, H. Eisaki, N. Hiraoka, H. Ishii, and K.-D. Tsuei, *Phys. Rev. B* **82**, 125123 (2010).
- ²⁵D. A. Zocco, R. E. Baumbach, J. J. Hamlin, M. Janoschek, I. K. Lum, M. A. McGuire, A. S. Sefat, B. C. Sales, R. Jin, D. Mandrus, J. R. Jeffries, S. T. Weir, Y. K. Vohra, and M. B. Maple, *Phys. Rev. B* **83**, 094528 (2011).
- ²⁶G. Garbarino, R. Weht, A. Sow, A. Sulpice, P. Toulemonde, M. Álvarez-Murga, P. Strobel, P. Bouvier, M. Mezouar, and M. Núñez-Regueiro, *Phys. Rev. B* **84**, 024510 (2011).
- ²⁷W. Lu, J. Yang, X. L. Dong, Z. A. Ren, G. C. Che, and Z. X. Zhao, *New J. Phys.* **10**, 063026 (2008).
- ²⁸Y. Takabayashi, M. T. McDonald, D. Papanikolaou, S. Margadonna, G. Wu, R. H. Liu, X. H. Chen, and K. Prassides, *J. Am. Chem. Soc.* **130**, 9242 (2008).
- ²⁹W. Bi, H. B. Banks, J. S. Schilling, H. Takahashi, H. Okada, Y. Kamihara, M. Hirano, and H. Hosono, *New J. Phys.* **12**, 023005 (2010).
- ³⁰X. L. Dong, W. Lu, J. Yang, W. Yi, Z. C. Li, C. Zhang, Z. A. Ren, G. C. Che, L. L. Sun, F. Zhou, X. J. Zhou, and Z. X. Zhao, *Phys. Rev. B* **82**, 212506 (2010).
- ³¹R. Khasanov, S. Sanna, G. Prando, Z. Shermadini, M. Bendele, A. Amato, P. Carretta, R. De Renzi, J. Karpinski, S. Katrych, H. Luetkens, and N. D. Zhigadlo, *Phys. Rev. B* **84**, 100501(R) (2011).
- ³²R. Kumai, N. Takeshita, T. Ito, H. Kito, A. Iyo, and H. Eisaki, *J. Phys. Soc. Jpn.* **78**, 013705 (2009).
- ³³K. Tatsumi, N. Fujiwara, H. Okada, H. Takahashi, Y. Kamihara, M. Hirano, and H. Hosono, *J. Phys. Soc. Jpn.* **78**, 023709 (2009).
- ³⁴K. Miyoshi, Y. Takaichi, Y. Takamatsu, M. Miura, and J. Takeuchi, *J. Phys. Soc. Jpn.* **77**, 043704 (2008).
- ³⁵K. Miyoshi, Y. Takaichi, E. Mutou, K. Fujiwara, and J. Takeuchi, *J. Phys. Soc. Jpn.* **78**, 093703 (2009).
- ³⁶A. Martinelli, M. Ferretti, P. Manfrinetti, A. Palenzona, M. Tropeano, M. R. Cimberle, C. Ferdeghini, R. Valle, M. Putti, and A. S. Siri, *Super. Sci. Tech.* **21**, 095017 (2008).
- ³⁷S. E. R. Hiscoks and J. B. Mullin, *J. Mater. Sci.* **4**, 962 (1969).
- ³⁸A. Ghoshray, B. Pahari, M. Majumder, M. Ghosh, K. Ghoshray, B. Bandyopadhyay, P. Dasgupta, A. Poddar, and C. Mazumdar, *Phys. Rev. B* **79**, 144512 (2009).
- ³⁹Z. A. Ren, J. Yang, W. Lu, W. Yi, G. C. Che, X. L. Dong, L. L. Sun, and Z. X. Zhao, *Mater. Res. Inno.* **8**, 105 (2008).
- ⁴⁰C. Tarantini, A. Gurevich, D. C. Larbalestier, Z.-A. Ren, X.-L. Dong, W. Lu, and Z.-X. Zhao, *Phys. Rev. B* **78**, 184501 (2008).
- ⁴¹R. H. Liu, G. Wu, T. Wu, D. F. Fang, H. Chen, S. Y. Li, K. Liu, Y. L. Xie, X. F. Wang, R. L. Yang, L. Ding, C. He, D. L. Feng, and X. H. Chen, *Phys. Rev. Lett.* **101**, 087001 (2008).
- ⁴²M. Mito, M. Hitaka, T. Kawae, K. Takeda, T. Kitai, and N. Toyoshima, *Jpn. J. Appl. Phys.* **40**, 6641 (2001).
- ⁴³H. Nakamura and M. Machida, *Phys. Rev. B* **80**, 165111 (2009).
- ⁴⁴T. Nomura, S. W. Kim, Y. Kamihara, M. Hirano, P. V. Sushko, K. Kato, M. Takata, A. L. Shluger, and H. Hosono, *Supercond. Sci. Technol.* **21**, 125028 (2008).
- ⁴⁵J. Zhao, Q. Huang, C. de la Cruz, S. Li, J. W. Lynn, Y. Chen, M. A. Green, G. F. Chen, G. Li, Z. Li, J. L. Luo, N. L. Wang, and P. Dai, *Nat. Mater.* **7**, 953 (2008).
- ⁴⁶K. Miyazawa, K. Kihou, P. Shirage, C. H. Lee, H. Kito, H. Eisaki, and A. Iyo, *J. Phys. Soc. Jpn.* **78**, 034712 (2009).
- ⁴⁷N. Takeshita *et al.* (unpublished).